SRTTU

JCARME
ISSN: 2228-7922

Journal of Computational and Applied Research
in Mechanical Engineering
Vol. 5, No. 2, pp. 97-109, Spring-Summer 2016
http://jcarme.srttu.edu

Effects of temperature gradient magnitude on bending angle in laser forming process of aluminium alloy sheets

Amir H. Roohi[a], H. Moslemi Naeini[b,*], M. Hoseinpour Gollo[c], J. Shahbazi Karami[c] and Sh. Imani Shahabad[a]

[a]*Department of Mechanical Engineering, Faculty of Engineering, Tarbiat Modares University, Tehran, I.R. Iran*
[b]*Department of Mechanical Engineering, Faculty of Engineering, Tarbiat Modares University, P.O.Box 14115/143, Tehran, I.R. Iran*
[c]*Department of Mechanical Engineering, Shahid Rajaee Teacher Training University (SRTTU), Lavizan, Tehran, Iran*

Article info:
Received: 26/09/2015
Accepted: 07/12/2015
Online: 03/03/2016

Keywords:
Laser forming process,
Aluminum alloy sheet,
Temperature gradient,
Bending angle,
Process parameters.

Abstract

Laser forming is a thermal forming process which uses laser beam irradiation to produce the desired final forms. In this article, the effect of temperature gradient across Al 6061-T6 aluminum sheets on bending angle is studied. Input parameters including laser power, scan velocity, beam diameter, and sheet thickness are the effective process parameters which influence the temperature gradient. Thus, a set of 81 numerical simulations based on a full factorial design with varying parameters is carried out and temperature gradient across the sheet thickness is measured. Effects of each input parameter on temperature gradient are determined using analysis of variance. Also, an equation is derived which predicts the temperature gradient for any arbitrary input parameter. The validity of the equation is done by comparing actual and predicted results. Numerical simulation is validated by experimental tests, which show a very close agreement. Finally, the effects of temperature gradient for three different sheet thicknesses on a final bending angle are derived. Results demonstrate that increase in temperature gradient across sheet thickness leads to increase in bending angle.

Nomenclature

	Bending angle
d	Beam diameter
P	Laser power
t	Sheet thickness
Ts	Sheet temperature
ΔT	Temperature gradient
hc	Heat transfer coefficient
q	Rate of heat loss per unit area
T	Environment temperature
v	Scan velocity

[*]*Corresponding author*
Email address: moslemi@modares.ac.ir

1. Introduction

2D laser forming (LF) process uses laser beam irradiation to produce bending angle in metallic and non-metallic sheets. Because of a steep temperature gradient along the sheet thickness, thermal stresses are induced in the irradiated zone and plastic deformation is produced. After the laser beam scan passes, the workpiece begins to cool and, as a result, a permanent bending angle is developed. Similar to flame

bending, sheet forming occurs due to thermal residual stresses instead of applying external mechanical forces. Thus, laser forming is a thermo-mechanical forming method [1]. A schematic image of LF is illustrated in Fig. 1. There are some advantages that make the laser forming method a new applicable process, which includes: (a) Compared with other thermal processes, laser beam focuses on a very small area and also high irradiation intensity could be achieved, (b) It is a non-contact forming process with a less amount of pollution, and (c) There is the possibility of forming the complicated shapes without using a hard tool, etc.

Laser forming has been extensively studied during recent years. Geiger and Vollertsen [2] identified three key mechanisms to explain the thermo-mechanical behaviors in laser forming including temperature gradient mechanism (TGM), buckling mechanism (BM), and shortening or planar upsetting mechanism (UM). Shichun, et al. [3] performed an experimental study on the effects of process parameters consisting of laser parameters, material properties, and sheet geometrical parameters on the bending angle of sheet metals. Guan Yanjin, et al. [4] developed a model to determine the influence of material properties on laser forming, which comprised Young's modulus, yield strength, thermal expansion coefficient, specific heat, and thermal conductivity. Che Jamil, et al. [5] conducted an analysis to investigate the effect of various rectangular laser beam geometries on the final product characteristics. They indicated that laser spot orientation significantly influenced the size of the heat zone in the workpiece and longer beam dimensions along the scanning line produced more deformation. Shen and Yao [6] investigated the mechanical characteristics of sheet metals before and after laser scan and found the residual compressive plastic strain as the most important reason for improving the fatigue strength of low-carbon steel after the laser forming process. Liu, et al. [7] studied the effect of the pre-stress and laser parameters on the negative bending of stainless foils loaded. Their experiments showed the angles increased significantly with pre-stress increases. Laser bending of brittle materials including, mono-crystalline silicon, borosilicate glass, and Al2O3 ceramic by CO2 CW laser and Nd:YAG pulsed laser was investigated by Dongjiang, et al. [8]. Results showed that elevated temperatures to prevent brittle fracture and selection of appropriate process parameters were required to achieve bending angle. Quadrini, et al. [9] studied the laser forming of open-cell aluminum foams and showed this process to be able to produce large deformations of the foam sheets without affecting their structural integrity. Knupfer, et al. [10] investigated the effects of laser forming on the mechanical and metallurgical properties of aluminum alloys (AA2024-T3) and low carbon steel (AISI1010). They utilized neutron diffraction for a range of laser line energies and a number of laser passes (one or three). Wang, et al. [11] carried out the simulation and prediction in laser bending of silicon sheet. The results indicated a hybrid mechanism in pulsed laser bending of silicon, rather than a simple mechanism of TGM or BM. Influence of different scan patterns of heating on laser forming of sheet metals was studied by Shi, et al. [12], who found that simultaneous heating on top and bottom surfaces with the same process parameters could lead to achieving negligible bending deformation and a uniform plastic plane strain field. Chakraborty, et al. [13] presented radial and circular paths to produce a bowl shape. They also studied the effect of laser power, beam diameter, and scan velocity on the bending angle of the bowls. The maximum bending angle was achieved at small beam diameter, high power, and low scanning velocity. Maji, et al. [14] conducted an experimental investigation and statistical analysis of pulsed laser bending of AISI 304 stainless steel sheet. They found that bending angle increased with the increase in laser power and pulse duration and decreased with an increase in the laser scan velocity. The effect of some process parameters, such as shielding gas and material properties, was investigated by Shidid, et al. [15]. They found that inert gas shielding could be used as a means of reducing oxidation in Grade-2 titanium sheets. Kim, et al. [16] proposed methods to reduce the

computational time and predict the deformed shapes in 3D laser forming. Results were used to determine the required deformations to form a 3D shape from a flat sheet metal using plane patches. Roohi, et al. [17] used external force-assisted laser forming to enhance the bending magnitude. Results demonstrated that about one-third of the final forming was due to applying external mechanical force. Also, random-based modeling of closed-cell aluminum foams was developed by Roohi, et al [18]. This model was used to predict the behavior of this type of materials during the laser forming process. Thermal stress analysis of sheet metals during the laser forming process was carried out by Yilbas and Akhtar [19], who found that the self-annealing effect of the laser scanning tracks could affect the stress fields and displacement in the workpiece. Hong Shen et al. [20] investigated the effects of cooling condition on the laser forming of stainless steel sheets in water and air. The highest bending angle was achieved when the upper surface was in the air and the bottom surface was immersed in water. Roohi et al. [21] investigated the laser forming process of Al6061-T6 sheets using a graphite spraying method to enhance the absorption coefficient and produce the bending angle in aluminum sheets. Safari et al. [22] employed a spiral irradiating scheme to achieve a 3D saddle shape in the laser forming process. Effects of spiral parameters including pitch of spiral, number of spirals, and direction of movement were determined for the curvature of the final shape. Wang et al. [23] used a scanning path planning, based on the geometrical curvature along the tube curves, for laser bending of a straight tube into a curved tube, both in plane and three-dimensional bending.

In this article, the focus is on determining the effects of temperature gradient (TG) magnitude on the final bending angle for three sheet thicknesses, which has not been investigated before. It should be mentioned that temperature gradient is defined as the difference of temperature between the irradiated and opposite surfaces. The results show a direct relationship between temperature gradient and forming magnitude. Also, an equation which shows the exact magnitude of bending angle based on the input temperature gradient is derived. In addition, the effects of four parameters, including laser power, scan velocity, number of scan passes, and sheet thickness, on the temperature gradient of aluminum alloy sheets are determined by means of analysis of variance (ANOVA). Results show that, among the input parameters, laser power and sheet thickness have a direct effect, and scan velocity and beam diameter have a reverse effect on the temperature gradient magnitude. Experimental tests are also carried out to validate the numerical simulations. Comparison between actual and numerical results shows a very good agreement.

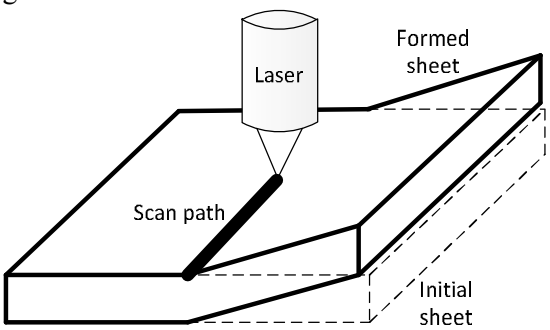

Fig. 1. Schematic image of laser forming.

2. Numerical approach

Numerical simulations of laser forming process are carried out to find out how temperature gradient magnitude affects bending angle. Process parameters are selected at such levels that temperature gradient mechanism is the active one. Thus, laser parameters produce a permanent bending angle without any melt occurrence on workpieces.

2. 1. Process theory

Temperature gradient mechanism is the most common mechanism used in LF process. Because of the relatively rapid heating of the sheet surface by a laser beam and slow thermal conduction to the lower layers (especially, in thicker sheets), a large temperature gradient develops in the thickness direction of the sheet.

At the beginning of the process, the sheet experiences a bending away from the laser beam which is called counter bending (Fig. 2 (a)). Further heating causes a decrease of mechanical strength in the heated zone. When thermal strains reach the maximum elastic strains, further thermal expansion is converted into the plastic compressive strains, because free thermal expansion of the heated zone is limited by the surrounding zone. In the cooling process, upper layers contract and also endure localized shortening due to compressive stresses, which results in a permanent bending angle toward the laser beam, as shown in Fig. 2 (b) [17].

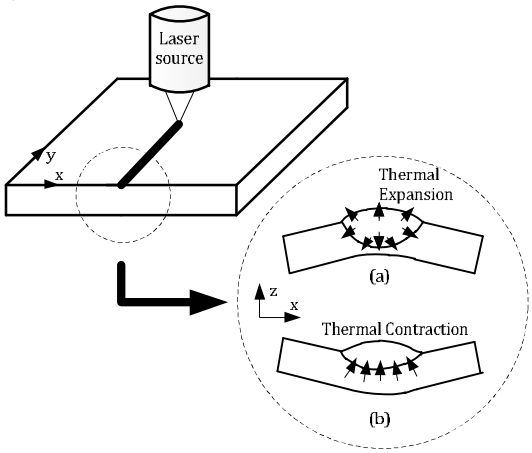

Fig. 2. Laser forming process steps using TGM, (a) Heating process (counter bending); (b) Cooling process (permanent bending angle).

2. 2. Geometrical model

The metal sheets are modeled as 3D and deformable parts. Sheets with the dimension of 100×50 (mm) and three thicknesses including 3, 4, and 5 (mm) are considered to see the effects of temperature gradients at different sheet thicknesses. An image of a typical sheet is illustrated in Fig. 3. Circles on the upper layer are the area to which the surface heat flux of the laser beam is applied. The distance between two adjacent circles was investigated by Labeas [24] and selected equal to the circles radius as an optimum quantity.

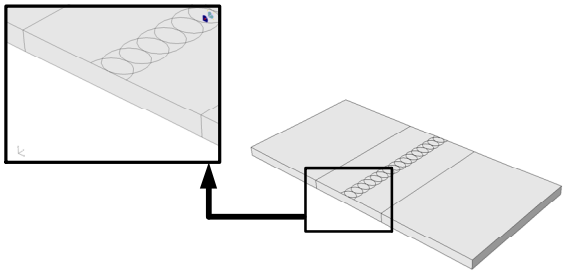

Fig. 3. Geometrical model of the sheet metal.

2. 3. Material data and assumptions

Al-6061 alloy temperature dependent properties are assigned to the finite element model used in this work. Physical and mechanical properties of Al-6061 alloy including thermal conductivity, density, Young's modulus, etc. are given in Table 1. The assumptions made for the material behavior and process conditions in numerical simulation are as follows:

1. The aluminum sheet materials are isotropic with strain-hardening;
2. The von Mises criterion is used as the yield criterion;
3. No surface melt occurs;
4. There are no external forces during the process;
5. Heat flux distribution is uniform in the irradiation area;
6. Initial sheet is considered flat with a uniform thickness; and
7. There is no residual stress.
8.

2. 4. Boundary condition

It is necessary to restrict the aluminium sheet movements during the process. So, cantilevered clamps are applied to the one end of the sheet. Thermal boundary condition is modeled by natural heat radiation and in a form of heat loss by free convection and conduction from the workpiece to the surrounding area. Convection follows Newton's law, the rate of the heat loss of heat per unit area in W/m2 due to convection is;

$$q=hc(Ts-T) \quad (1)$$

Where hc is the heat transfer coefficient, Ts the sheet temperature and T is the environment temperature, which is set as 25 C.

The rate of the heat per unit area in W/m2 due to radiation is;

Table 1. Temperature dependent material properties for 6061-T6 aluminum alloy [25].

Temperature	°C	37.8	148.9	260	315.6	426.7
Thermal Conductivity	W/m°C	0.0162	0.0184	0.0201	0.0207	0.0223
Heat Capacity	J/kg°C	945	1004	1052	1078	1133
Density	Kg/m3	2685	2667	2657	2630	2602
Young's Modulus	GPa	68.54	63.09	53.99	47.48	31.72
Yield Strength	MPa	274.4	248.2	159.7	66.2	17.9
Thermal Expansion	μ/°C	23.45	25.67	27.56	28.53	30.71

$$q=5.67\times10\text{-}8(Ts4\text{-}T4) \quad (2)$$

where ε is the surface emissivity [26].

2. 5. Elements and Mesh

For the process analysis, the element type 'C3D8RT' in ABAQUS software is used, which is an 8-node thermally coupled brick, trilinear displacement and temperature, reduced integration, hourglass control (see Fig. 4). A dense FE mesh is selected in the critical parts around the laser beam path and the heat-affected zone.

These volumes are estimated to extend in a zone of width equal to five times of the laser beam diameter. A gradual increase of the element size from the laser path to the sheet edges is selected in non-critical parts. A mesh study to find the appropriate mesh size is carried out. Bigger mesh sizes decrease the accuracy of the results and smaller sizes significantly increase the simulation runtime with a negligible change in the results. Regarding this concept, global mesh size is considered equal to 0.5mm in the dense meshed part. Noncritical parts are considered the zones far from the heat-affected zone. Also, five meshes along the sheet thickness are considered to have a better understanding of the temperature gradient. Sheet free edge displacement and temperature distribution contours at the end of the LF process (after 350 sec of cooling time) are illustrated, respectively, in Fig. 5 and Fig. 6. Note that these contours are from an aluminum sheet with the thickness of 4mm nd process parameters have the laser power of 1250 W, scan velocity of 1m/min, and laser beam diameter of 6 mm. A cross-section of the sheet through the bending line is performed and the highest temperature gradient through this cross-section is measured during the laser forming process. These results are used to determine the effect of temperature gradient.

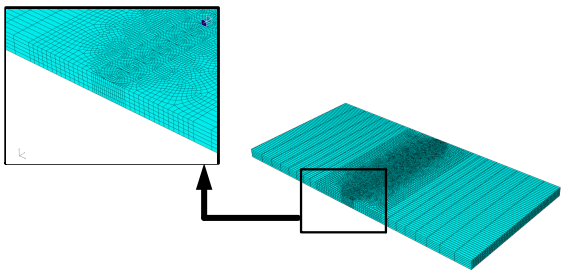

Fig. 4. Aluminum sheet meshing.

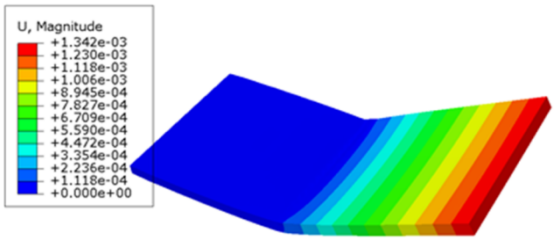

Fig. 5. Free edge displacement of the sheet (1:10 scale).

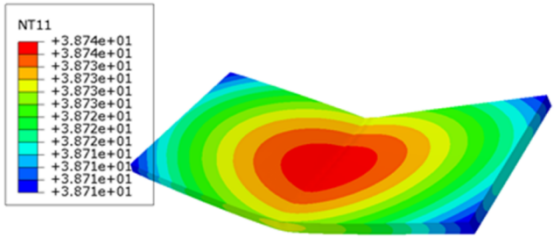

Fig. 6. Temperature distribution contour of the sheet (1:10 scale).

Table 2. Input parameters and their levels.

Parameter	Symbol	Unit	Low level	Mid-level	High level
Laser power	P	W	1125	1250	1375
Scan velocity	v	m/min	0.9	1.0	1.1
Beam diameter	d	mm	5	6	7
Sheet thickness	t	mm	3	4	5

2. 6. Numerical Simulation Plan

Numerical simulations are carried out based on a full factorial design of experiments to include all the possible experiments that would be $n=m^f=3^4=81$ run; where m is the number of levels and f is input parameters. Input parameters and their levels are listed in Table 2. The levels are selected in such a way that the active mechanism of laser forming is temperature gradient, i.e. producing a steep temperature gradient along the sheet thickness.

3. Experimental Procedure

Laser forming experiments were carried out on Al-6061-T6 alloy sheets to validate the accuracy of the numerical approach.

The size of the aluminums samples was 100×50 mm with different thicknesses, which was cut by the wire cut machine (Fig. 7). One side of the aluminums sheets was free to move without restrictions and the opposite side was completely fixed in all directions. A pulsed CO_2 laser (model Bystronic-Bysprint 3015) with maximum mean laser power of 1800 W was utilized. The beam diameter through the experiments was set equal to 1 mm. The bending angle was measured by a CMM Mora3 with the accuracy of 2.2 microns + L/300. The procedure of measuring bending angle was that the spatial position of 3 points on each of the bending planes was determined. Then, the final bending angle was the angle between two imaginary planes which passed through these determined 3 points. This process was carried out by Inca 3D software. The bent aluminum sheet in the final experiment is shown in Fig 8. In order to increase the laser absorption coefficient of the aluminum sheets, the sheet was coated with a graphite spray every three passes.

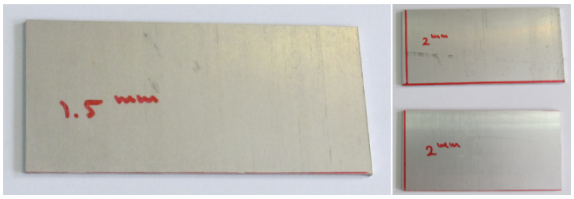

Fig. 7. Aluminum samples with different thicknesses.

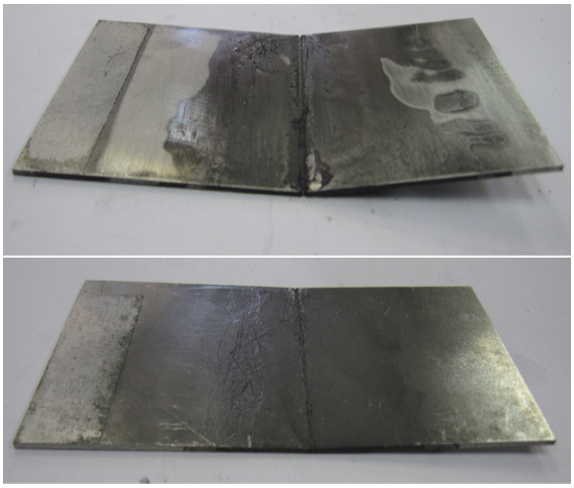

Fig. 8. Images of laser formed aluminum sheets.

3. 1. Validation results

Effects of the changes of one input parameter on the bending angle, when other input parameters were set constant, were investigated in the experiments. The comparison between the numerical and experimental results is shown in Fig. 9 (a-d). The results revealed a close agreement between the experiments and FE predictions of the deformation behavior of the sheets. A slight discrepancy existed, since the finite element model was perfectly homogeneous and free of material inhomogeneity and impurities, which are commonly observed in metal sheets.

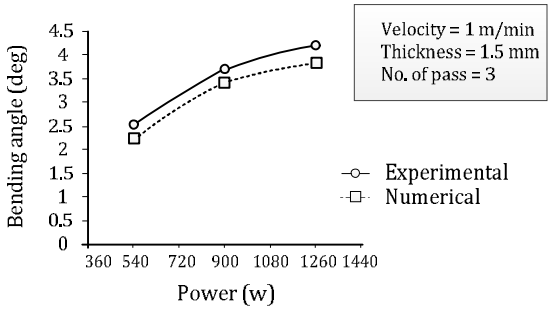

(a) Effect of laser power on bending angle

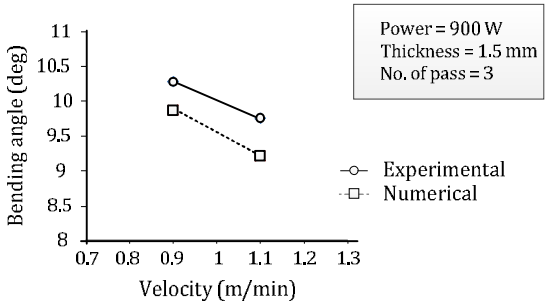

(b) Effect of scan velocity on bending angle

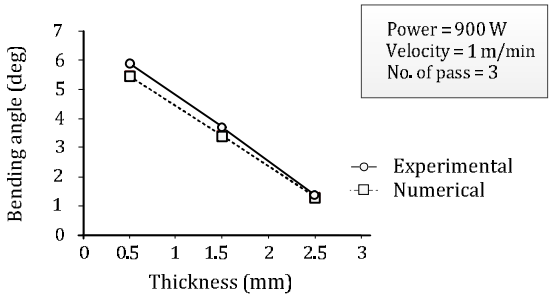

(c) Effect of sheet thickness on bending angle

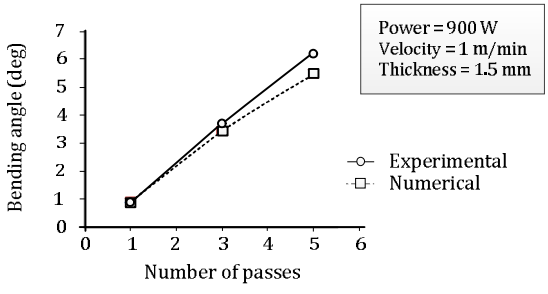

(d) Effect of the number of scan passes on bending angle

Fig. 9. Comparison between experimental and simulation results.

4. Results and discussion

4. 1. Effects of temperature gradient

Three different sheet thicknesses is considered to see how the temperature gradient influences on a final bending angle. Sheet thickness is separated from other process parameters because of its contrast effects, which (a) from strength of materials perspective, when thickness increases the flexural rigidity increases, that needs bigger stresses to bend a thicker sheet. Therefore, sheet thickness has a negative effect on bending sheet metals in the laser forming process; (b) from the thermal effects perspective, when thickness increases the temperature gradient across the thickness increases due to increase in sheet volume and less effect of thermal conductivity to distribute the temperature. Thus, the temperature gradient in thicker sheet is higher and it helps to bend the sheet in laser forming. Note that to measure the maximum temperature gradient in each numerical run, the highest temperature of all the nodes located in laser scan path is identified and differences between the temperature of top and bottom layer at this point is measured. The effects of the temperature gradient magnitude on final bending angle for three mentioned thicknesses are illustrated in Fig. 10 (a-c). The quantitative effects of each are determined by equations (3) - (5).

$$\alpha=0.0031\Delta T+0.899 \quad (t = 3 \text{ mm}) \tag{3}$$

$$\alpha=0.0055\Delta T-0.502 \quad (t = 4 \text{ mm}) \tag{4}$$

$$\alpha=0.0034\Delta T-0.554 \quad (t = 5 \text{ mm}) \tag{5}$$

where α is bending angle (degree) and ΔT is temperature gradient across thickness (°C).
An increase in the temperature gradient means there was higher temperature differences between top and bottom layers of the sheet. In fact, high non-permanent counter bending occurs due to high temperature gradient. Because of the decreased mechanical strength in the heated zone and simultaneous increase in the magnitude of counter bending, a higher compressive plastic strain was applied to the irradiated zone. During the cooling process,

upper layers contracted and also endured bigger localized shortening due to the higher compressive stresses caused by the elastic deformation of the surrounding zone. Thus, the higher temperature gradient led to increase in the final bending angle.

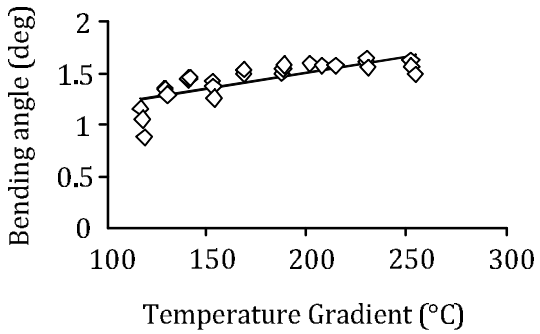

(a) Effect of TG for the sheet thickness of 3 mm

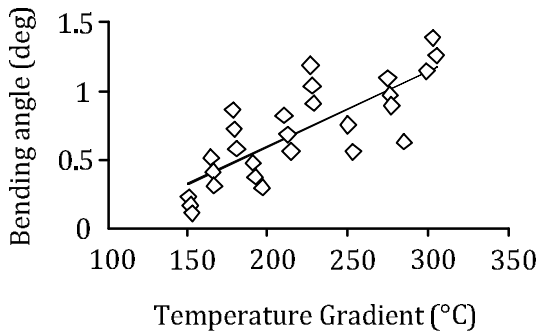

(b) Effect of TG for the sheet thickness of 4 mm

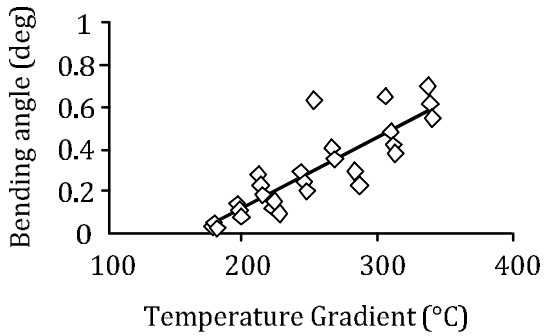

(c) Effect of TG for the sheet thickness of 5 mm

Fig. 10. Effect of temperature gradient on the final bending angle.

4. 2. Effects of process parameters

The effects of each process parameter on the temperature gradient magnitude are shown in Figs. 11-14. These effects are indirectly in accordance with many investigation results such as [3], [27], [28], etc. Figure 11 shows that, when the laser power increased, temperature gradient increased. In fact, when laser power increased, higher input thermal energy was distributed in the irradiation area. Thus, the upper layer of the sheet became warmer and, despite thermal conductivity, the temperature gradient increased.

Figure 12 illustrates that the scan velocity, in the defined range of changes, had a negligible effect and decreased the temperature gradient with a slight slope, because when the scan velocity increased, the duration of laser irradiation at every point decreased, so it had a lower thermal effect. The effect of beam diameter on the temperature gradient, with a quadratic curve, is shown in Fig. 13.

It is obvious when the beam diameter decreased, laser thermal energy intensity induced on the irradiation area increased (note that laser power was assumed to be constant). Thus, the decrease in beam diameter increased the temperature gradient; however, an excessive decrease in beam diameter was not very helpful to increase the temperature gradient and, as a consequence, to increase bending angle, because excessive thermal energy intensity led to the melting of sheet surface and, finally, cut the sheet metal. The effects of sheet thickness on the temperature gradient magnitude are illustrated in Fig. 14.

As is explained previously, an increase in the sheet thickness caused an increase in the sheet volume, so thermal conductivity had a lower effect on the heat transfer of hot upper layer; as a result, the temperature gradient increased. Furthermore, interacted effects of input parameters on the final forming magnitude are illustrated in Figs. 15-20. Thus, as discussed before, an increase in laser power increased both temperature gradient and bending angle. Also, the decrease in velocity and beam diameter finally led to an increase in bending angle.

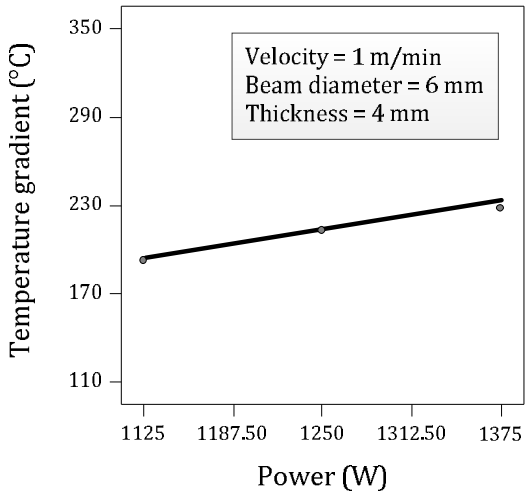

Fig. 11. Effect of laser power on TG.

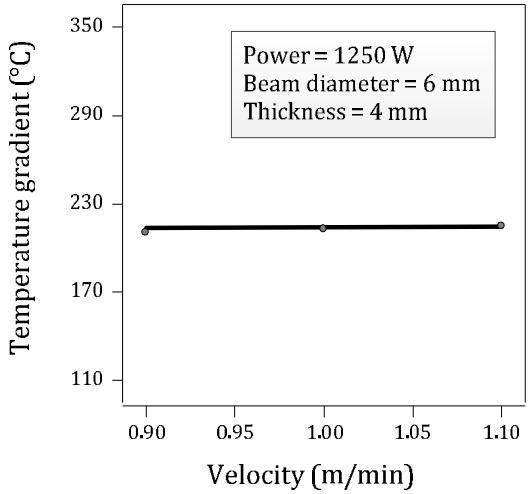

Fig. 12. Effect of scan velocity on TG.

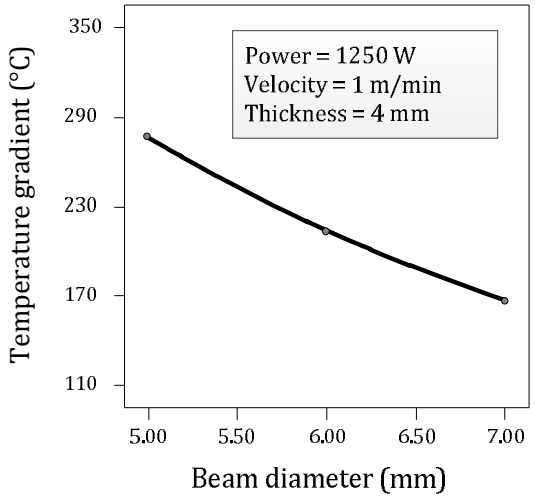

Fig. 13. Effect of beam diameter on TG.

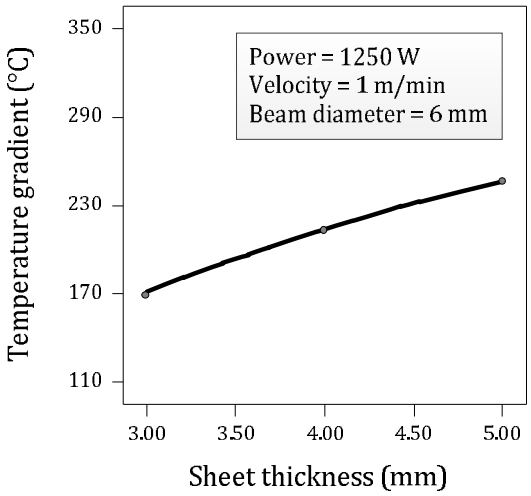

Fig. 14. Effect of sheet thickness on TG.

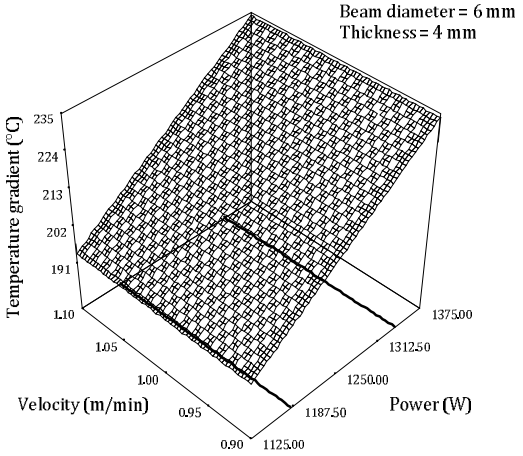

Fig. 15. Effect of laser power and scan velocity on TG.

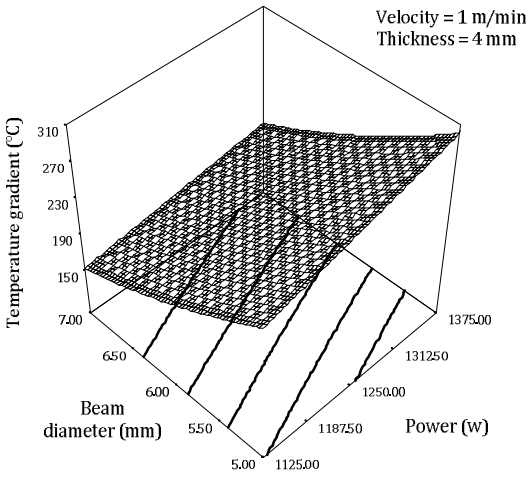

Fig. 16. Effect of laser power and beam diameter on TG.

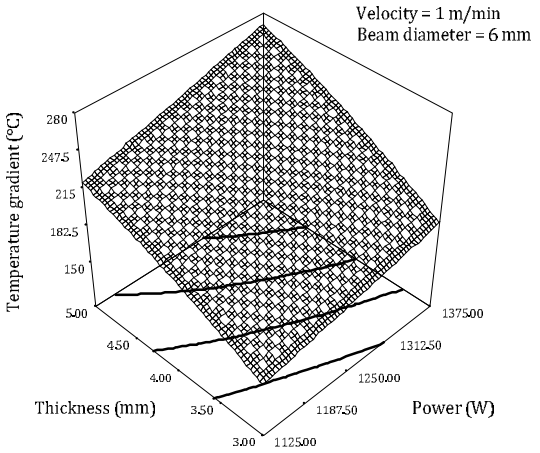

Fig. 17. Effect of laser power and sheet thickness on TG.

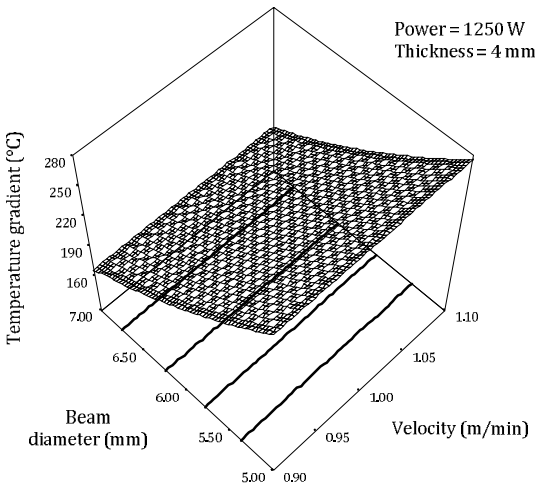

Fig. 18. Effect of scan velocity and beam diameter on TG.

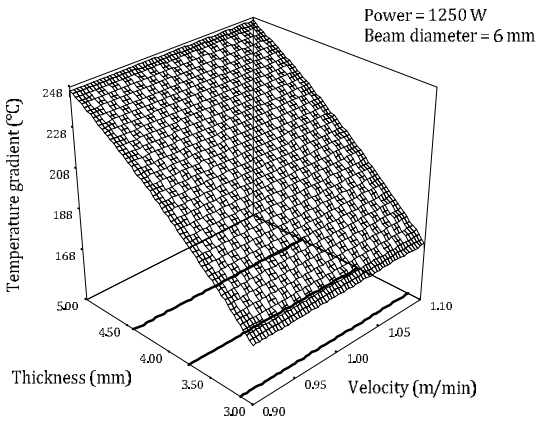

Fig. 19. Effect of scan velocity and sheet thickness on TG.

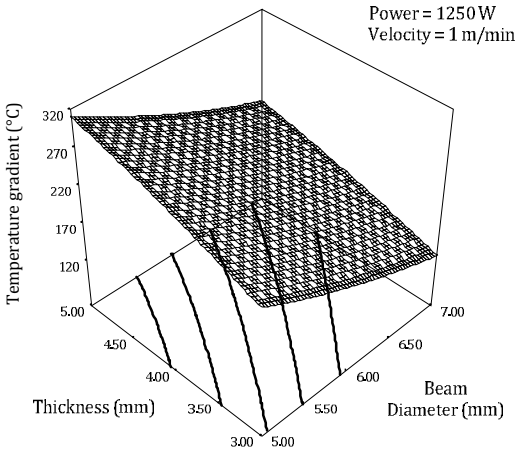

Fig. 20. Effect of beam diameter and sheet thickness on TG.

4. 3. Predicting temperature gradient magnitude

The temperature gradient magnitude along the thickness of aluminum sheets based on input parameters is determined in Eq. (6).

$$\Delta T=185.905+0.281\times P+1.707\times v-87.128\times d+50.285\times t-0.043\times P\times d+0.034\times P\times t-2.644\times d\times t+8.092\times d^2-4.969\times t^2 \quad (6)$$

In the above equation, P is the laser power (W), v is scan velocity (m/min), d is beam diameter (mm), and t is sheet thickness (mm). The diagram of actual versus predicted values by Eq. (6) is illustrated in Fig. 21. The data point located by the 45 degree line approved the validity of the derived equation.

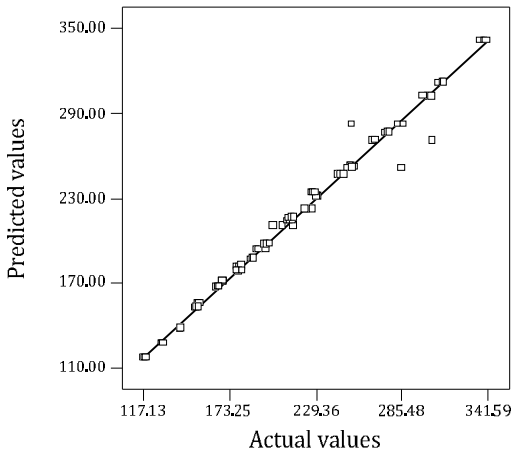

Fig. 21. The graph of the actual versus predicted responses.

5. Conclusions

In this article, laser forming process of Al 6061-T6 aluminum sheets with three different thicknesses of 3, 4, and 5 mm was investigated. Using the full factorial design of the experiment, 81 numerical runs were carried out to find out how the four process parameters including laser power, scan velocity, beam diameter, and sheet thickness influenced the temperature gradient magnitude. For this reason, an equation was derived to predict the temperature gradient. Afterwards, the three equations were presented which calculated the final bending angle for each of the three sheet thicknesses regarding the TG magnitude. In general, to enhance the highest bending angle, all the attempts were made to increase the temperature gradient magnitude. Thus, an increase in laser power and a simultaneous decrease in the scan velocity and beam diameter had an effective influence to achieve the highest forming magnitude for the aluminum sheets. Results showed that:

1. Increased temperature gradient from 119.01°C to 252.21°C at the sheet thickness of 3 mm led to an increase in the final bending angle from 0.883° to 1.638°.
2. In the aluminum sheets with the thickness of 4 mm, the final bending angle changed from 0.114° to 1.393° when the temperature gradient varied from 153.32°C to 303.24°C.
3. In the aluminum sheets with the thickness of 5 mm, an increase in temperature gradient from 181.54°C to 337.29°C resulted in the increased final bending angle from 0.023° to 0.702°.
4. Maximum bending angle of 1.638° was for the minimum sheet thickness and its relevant maximum temperature gradient.
5. When laser power increased, the temperature gradient increased, i.e. when power changed from 1125 W to 1375 W, temperature gradient raised from 193.95°C to 227.90°C.
6. Scan velocity changes had a negligible effect on the temperature gradient magnitude.
7. When the beam diameter increased, the temperature gradient decreased with a steep slope, i.e. when the diameter varied from 5 mm to 7 mm, temperature gradient changed from 276.54°C to 166.12°C.
8. When sheet thickness increased, the temperature gradient increased with a quadratic trend. In other words, when sheet thickness changed from 3 mm to 5 mm W, temperature gradient raised from 167.84°C to 245.85°C.
9. Maximum temperature gradient of 340.97°C was achieved by maximizing laser power, scan velocity, and sheet thickness and simultaneously minimizing beam diameter.

References

[1] X. Zhang, *Laser-assisted High Precision Bending and its Applications*, Ph.D. Thesis, Purdue University, (2004).

[2] M. Geiger, and F. Vollertsen, "The Mechanisms of Laser Forming", *CIRP Annals - Manufacturing Technology*, Vol. 42, No. 1, pp. 301-304, (1993).

[3] W. Shichun, and Z. Jinsong, "An experimental study of laser bending for sheet metals", *Journal of Materials Processing Technology*, Vol. 110, No. 2, pp. 160-163, (2001).

[4] Y. Guan, S. Sun, G. Zhao, and Y. Luan, "Influence of material properties on the laser-forming process of sheet metals", *Journal of Materials Processing Technology*, Vol. 167, No. 1, pp. 124-131, (2005).

[5] M. S. Che Jamil, M. A. Sheikh, and L. Li, "A study of the effect of laser beam geometries on laser bending of sheet metal by buckling mechanism", *Journal of Optics & Laser Technology*, Vol. 43, No. 1, pp. 183-193, (2011).

[6] H. Shen, and Z. Yao, "Study on mechanical properties after laser forming", *Journal of Optics and Lasers in Engineering*, Vol. 47, No. 1, pp. 111-117, (2009).

[7] J. Liu, S. Sun, Y. Guan, and Z. Ji, "Experimental study on negative laser bending process of steel foils", *Journal of Optics and Lasers in Engineering*, Vol. 48, No. 1, pp. 83-88, (2010).

[8] D. Wu, Q. Zhang, G. Ma, Y. Guo, and D. Guo, "Laser bending of brittle materials", *Journal of Optics and Lasers in Engineering*, Vol. 48, No. 4, pp. 405-410, (2010).

[9] F. Quadrini, A. Guglielmotti, E. A. Squeo, and V. Tagliaferri, "Laser forming of open-cell aluminium foams", *Journal of Materials Processing Technology*, Vol. 210, No. 11, pp. 1517-1522, (2010)

[10] S. M. Knupfer, and A. J. Moore, "The effects of laser forming on the mechanical and metallurgical properties of low carbon steel and aluminium alloy samples", *Journal of Materials Science and Engineering*: *A*, Vol. 527, No. 16-17, pp. 4347-4359, (2010)

[11] X. -Y. WANG, W. -X. XU, W. -J. XU, Y. -F. HU, Y. -D. LIANG, and L. -J.WANG, "Simulation and prediction in laser bending of silicon sheet", *Transactions of Nonferrous Metals Society of China*, Vol. 21, pp. 188-193, (2011).

[12] Y. Shi, Y. Liu, P. Yi, and J. Hu, "Effect of different heating methods on deformation of metal plate under upsetting mechanism in laser forming", *Journal of Optics & Laser Technology*, Vol. 44, No. 2, pp. 486-491, (2012)

[13] S. Shekhar Chakraborty, V. Racherla, and A. Kumar Nath, "Parametric study on bending and thickening in laser forming of a bowl shaped surface" *Journal of Optics and Lasers in Engineering*, Vol. 50, No. 11, pp. 1548-1558, (2012)

[14] K. Maji, D. K. Pratihar, and A.K. Nath, "Experimental investigations and statistical analysis of pulsed laser bending of AISI 304 stainless steel sheet", *Journal of Optics & Laser Technology*, Vol. 49, pp. 18-27, (2013).

[15] D. P. Shidid, M. H. Gollo, M. Brandt, and M. Mahdavian, "Study of effect of process parameters on titanium sheet metal bending using Nd: YAG laser", *Journal of Optics & Laser Technology*, Vol. 47, pp. 242-247, (2013).

[16] J. Kim, and S. Na, "3D laser-forming strategies for sheet metal by geometrical information", *Journal of Optics & Laser Technology*, Vol. 41, No. 6, pp. 843-852, (2009).

[17] A. H. Roohi, M. H. Gollo, and H. M. Naeini, "External force-assisted laser forming process for gaining high bending angles", *Journal of Manufacturing Processes*, Vol. 14, No. 3, pp. 269-276, (2012).

[18] A. H. Roohi, M. H. Naeini, M. H. Gollo, M. Soltanpour, and M. Abbaszadeh, "On the random-based closed-cell metal foam modeling and its behavior in laser forming process", *Journal of Optics & Laser Technology*, Vol. 72, pp. 53-64, (2015).

[19] B. S. Yilbas, and S. S. Akhtar, "Laser bending of metal sheet and thermal stress analysis", *Journal of Optics & Laser Technology*, Vol. 61, pp. 34-44, (2014).

[20] H. Shen, M. Ran, J. Hu, and Z. Yao, "An experimental investigation of underwater pulsed laser forming", *Journal of Optics and Lasers in Engineering*, Vol. 62, pp. 1-8, (2014).

[21] A. H. Roohi, H. M. Naeini, and M. H. Gollo, "An experimental investigation of parameters effect on laser forming of Al6061-T6 sheets", *Proceedings of the Institution of Mechanical Engineers, Part L: Journal of Materials Design and Applications,* (2015).

[22] M. Safari, and M. Farzin, "Experimental investigation of laser forming of a saddle shape with spiral irradiating scheme", *Journal of Optics & Laser Technology*, Vol. 66, pp. 146-15, (2015).

[23] X. Y. Wang, J. Wang, W. J. Xu, and D. M. Guo, "Scanning path planning for laser bending of straight tube into curve tube", *Journal of Optics & Laser Technology*, Vol. 56, pp. 43-51, (2014).

[24] G. N. Labeas, "Development of a local three-dimensional numerical simulation model for the laser forming process of aluminium components:, *Journal of Materials Processing Technology*, Vol. 207, No. 1–3, pp. 248-257, (2008).

[25] M. Awang, V. Mucino, Z. Feng, and S. David, "Thermo-Mechanical Modeling of Friction Stir Spot Welding (FSSW) Process: Use of an Explicit Adaptive Meshing Scheme", *SAE 2005 World Congress & Exibition*, (2005).

[26] M. Hoseinpour Gollo, S. M. Mahdavian, H. Moslemi Naeini, "Statistical analysis of parameter effects on bending angle in laser forming process by pulsed Nd:YAG laser", *Journal of Optics & Laser Technology*, Vol. 43, No. 3, pp. 475-482, (2011).

[27] S. P. Edwardson, E. Abed, C. Carey, K. Edwards, G. Dearden, and K. Watkins, "Factors influencing the bend per pass in multi-pass laser forming", *Proceedings of the 5th LANE 1*, pp. 557-568, (2007).

[28] S. P. Edwardson, E. Abed, K. Bartkowiak, G. Dearden, and K. G. Watkins, "Geometrical influences on multi-pass laser forming", *Journal of Physics D: Applied Physics*, Vol. 39, No. 2, pp. 382, (2006).